Thermal Behavior of J-Aggregates in a Langmuir−Blodgett Film of Pure Merocyanine Dye Investigated by UV−visible and IR Absorption Spectroscopy

Yoshiaki Hirano,* Shinsuke Tateno, Ari Maio, and Yukihiro Ozaki

Department of Chemistry, School of Science and Technology, Kwansei Gakuin University, 2-1 Gakuen, Sanda 669-1337, Japan

Received: September 16, 2008; Revised Manuscript Received: January 7, 2009

We have characterized the structure of J-aggregate in a Langmuir−Blodgett film of pure merocyanine dye (MS_{18}) fabricated under an aqueous subphase containing a cadmium ion (Cd^{2+}) and have investigated its thermal behavior by UV−visible and IR absorption spectroscopy in the range from 25 to 250 °C with a continuous scan. The results of both UV−visible and IR absorption spectra indicate that temperature-dependent changes in the MS_{18} aggregation state in the pure MS_{18} system are closely and mildly linked with the MS_{18} intramolecular charge transfer and the behavior of the packing, orientation, conformation, and thermal mobility of MS_{18} hydrocarbon chain, respectively. The J-aggregate in the pure MS_{18} system dissociates from 25 to 150 °C, and the dissociation temperature at 150 °C is higher by 50 °C than that in the previous MS_{18}-arachidic acid (C_{20}) binary system. The lower dissociation temperature in the binary system originates from the fact that temperature-dependent structural disorder of cadmium arachidate (CdC_{20}), being phase-separated from MS_{18}, has an influence on the dissociation of J-aggregate. From 160 to 180 °C, thermally induced blue-shifted bands, caused by the oligomeric MS_{18} aggregation, appear at around 520 nm in the pure MS_{18} system by contraries, regardless of the lack of driving force by the melting phenomenon of CdC_{20}. The temperature at which the 520 nm bands occur is in good agreement with the melting point (160 °C) of hydrocarbon chain in MS_{18} with Cd^{2+}, whereas its chromophore part is clearly observed to melt near 205 °C by UV−visible spectra. Therefore, it is suggested that the driving force that induces the 520 nm band in the pure MS_{18} system arises from the partial melting of hydrocarbon chain in MS_{18} with Cd^{2+}.

1. Introduction

In recent years, precise control of dye aggregation states in ultrathin films has been expected to be one of the significant research subjects in order to induce higher performance of photovoltaic cells, optical waveguides, and ultrafast optical switches that will probably be improved utilizing the ultrathin films containing dyes.[1−4] Consequently, we have been engaged in studies on the control of dye aggregation states using Langmuir−Blodgett (LB) films containing merocyanine dye with an octadecyl group ($n = 18$, MS_{18}, 3-carboxymethyl-5-[2-(3-octadecyl-benzothiazolin-2-ylidene)-ethylidene]rhodanine), see Figure 1),[5−10] since J- and H-aggregates are easily tuned in the MS_{18} LB films.[5−21] In previous papers, we examined the thermal behavior of J- and H-aggregates in mixed LB films of the MS_{18}-arachidic acid (C_{20}) binary and $MS_{18}-C_{20}$-*n*-octadecane (AL_{18}) ternary systems by means of UV−visible and IR absorption spectroscopy from 25 to 250 °C with a continuous scan.[5,10] From these studies, the following four guideposts have been deduced.[5,10]

First, it has been suggested that temperature-dependent changes in the MS_{18} aggregation state in both mixed systems are determined by the close structural linkage between the degree of MS_{18} intramolecular charge transfer and the behavior of MS_{18} hydrocarbon chain,[5,10] and that the variations in individual structures of MS_{18} and C_{20} in the ternary system are linked with the presence and evaporation of AL_{18} as well.[10] Second, the J- and H-aggregates dissociate from 25 to 100 °C and from 25 to 50 °C in the binary and ternary systems, respectively.[5,10] Third,

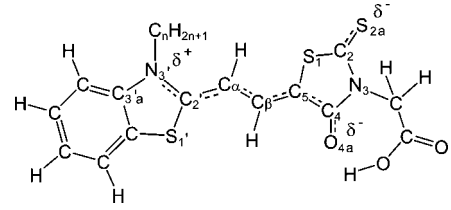

Figure 1. Chemical structure of merocyanine dye (MS_n) with an alkyl chain. The intramolecular charge transfer is schematically represented.

thermally induced blue-shifted bands, ascribed to the oligomeric MS_{18} aggregation, appear near 515 nm from 110 to 160 °C in both mixed systems.[5,10] Then, it has been suggested that the driving force that induces the 515 nm band arises from the melting phenomenon of cadmium arachidate (CdC_{20}) which is phase-separated from MS_{18} in as-deposited LB films.[10] Fourth, the degree of orthorhombic subcell packing of CdC_{20} being partly present in the majority of hexagonal natures in their domains in the ternary system is fairly less than that in the binary system.[5,10] Thus, these guidelines obtained by the comparison of above results are of great significance not only for the search of possibility of recontrol of dye aggregation state but also for the understanding of temperature-dependent structural variations in assembled molecules in basic research.

Furthermore, we investigate the thermal behavior of J-aggregate in a pure MS_{18} LB film with the continuous scan and compare the results of present pure MS_{18} system and previous $MS_{18}-C_{20}$ binary or $MS_{18}-C_{20}-AL_{18}$ ternary system, or both, to reveal the following four questions. First, are the temperature-

* To whom correspondence should be addressed. E-mail: baw91933@kwansei.ac.jp.

10.1021/jp808220w CCC: $40.75
Published on Web 02/10/2009

dependent changes in the MS_{18} aggregation state in the pure MS_{18} system closely linked with the degree of MS_{18} intramolecular charge transfer and the behavior of MS_{18} hydrocarbon chain as well, as has been mentioned in the previous mixed systems?[5,10] Second, is the dissociation temperature of J-aggregate in the pure MS_{18} system the same as that (100 °C) in the binary system?[5] Third, while we predict that the thermally induced blue-shifted bands in the pure MS_{18} system will not appear at around 515 nm at 110 °C because of absence of CdC_{20}, is this expectation valid? Fourth, is the melting phenomenon of MS_{18} chromophores coupled with a cadmium ion (Cd^{2+}) monitored in the pure MS_{18} system, although it could not clearly be seen in both mixed systems?[5,10] So far, no systematic study on the temperature-dependent structural characterization of J-aggregate in the pure MS_{18} system from these viewpoints has come to our knowledge.

This paper reports the results of structural characterization of J-aggregate in the pure MS_{18} LB film at room temperature (25 °C) and its thermal behavior by UV−visible and IR absorption spectroscopy in the range from 25 to 250 °C with the continuous scan. The present study provides new insights of (1) the differences in the degree of individual structural variations and linkages in MS_{18} and in the temperature range of the linkages between the present pure MS_{18} and previous MS_{18}−C_{20} binary systems and their reason, (2) the variation in dissociation temperature of J-aggregate in the pure MS_{18} and binary systems and its origin, (3) the fluctuation of temperature at which a thermally induced blue-shifted band appears between the pure MS_{18} and mixed systems and the switch of its driving force, and (4) the observation of melting phenomenon of MS_{18} chromophores with Cd^{2+} in the pure MS_{18} system and the reason for no observation of its melting in the mixed systems.

2. Experimental Section

2.1. Chemicals and Sample Preparation Procedures. Merocyanine dye with an octadecyl group (MS_{18}) was purchased from Hayashibara Biochemical Laboratories Inc. (Okayama, Japan), and was used without further purification. Spreading solution of the pure MS_{18} system was prepared using freshly distilled chloroform from DOJINDO Laboratories (Kumamoto, Japan). The MS_{18} concentration was on the order of 10^{-4} M. A USI system trough (Fukuoka, Japan) was used. The preparation of an aqueous subphase containing cadmium chloride ($CdCl_2$) and sodium hydrogencarbonate ($NaHCO_3$) was the same as that reported previously.[5−10] The subphase was kept at 20 °C during the surface pressure (π)-area (A) isotherm measurement and the film deposition. The π-A isotherm measurement of pure MS_{18} monolayer was performed at a compression rate of 0.0500 {Å^2/(molecule·sec)}. The monolayer was directly transferred onto CaF_2 substrate or gold-evaporated glass substrate by the vertical dipping method. The raising and dipping velocities of both substrates with the size of 13 × 38 mm^2 were 2.5 mm/min up to 3(×2) layers, and then 25 mm/min afterward. The number of layer of Y-type LB films deposited on both sides of substrates was 15(×2) layers. The transfer ratio of all the LB films was approximately unity.

Two samples were prepared to investigate the thermal behavior of pure MS_{18} LB film by UV−visible and IR transmission absorption spectroscopy. Before the measurements of their thermal behavior, it was confirmed that the MS_{18} aggregation states of two samples are the same, based on the results of their UV−visible spectra. All the UV−visible and IR absorption spectrum measurements were carried out immediately after the sample preparation.

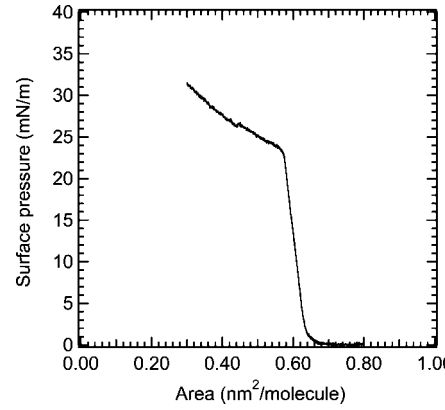

Figure 2. Surface pressure (π)-area (A) isotherm of monolayer of pure merocyanine dye with an octadecyl group (MS_{18}) on an aqueous subphase containing cadmium chloride ($CdCl_2$) and sodium hydrogencarbonate ($NaHCO_3$) at 20 °C.

2.2. Spectroscopic Measurements. The measurements of UV−visible transmission absorption spectra were performed using a Shimadzu UV-3101PC UV−vis spectrometer. IR transmission- and reflection−absorption spectra at room temperature (25 °C), and IR temperature-dependent transmission absorption spectra were recorded at a 4 cm^{-1} resolution by coadding 256 scans using a Nicolet Magna 560 FT-IR spectrometer equipped with an MCT detector and a Nicolet Magna 870 FT-IR spectrometer with a TGS detector, respectively. The IR spectrometer involving a sample chamber was purged with dry air.

The UV−visible and IR absorption spectrum measurements of a pure MS_{18} LB film at room temperature were carried out using nonpolarized light and polarized light. The polarized UV−visible and IR transmission spectra $A_{\parallel}$ and $A_{\perp}$ of the LB film were measured using linearly polarized light with the electric vector parallel and perpendicular to the raising and dipping directions of substrate, respectively. The IR reflection−absorption spectra of the LB film on gold-evaporated glass substrate were taken at the incident angle of 80° with the reflection attachment of Spectra Tech Inc. using p-polarized light.

The measurement system of temperature-dependent UV−visible and IR transmission spectra of LB film on the CaF_2 substrate was the same as that reported previously.[5,10] Both nonpolarized spectra were automatically collected at an interval of about 2 °C from 25 to 250 °C at a rate of approximately 0.4 °C /min.

2.3. Spectral Analyses. The analyses in temperature-dependent UV−visible and IR spectra were carried out by using homemade software. The third-derivative spectra were calculated by the Savitzky−Golay method.

3. Results and Discussion

3.1. Surface Pressure (π)-Area (A) Isotherm of Pure MS_{18} Monolayer. Figure 2 shows surface pressure (π)-area (A) isotherm of a pure MS_{18} monolayer on an aqueous subphase at 20 °C. The sudden upturn of surface pressure starts from the occupied area near 0.64 (nm^2/molecule). The area at 15 mN/m is 0.60 (nm^2/molecule), which is in good agreement with the value in the earlier work.[20] The result suggests that the long axis of MS_{18} chromophore is parallel to the air−water interface. Then, we can recognize that the surface pressure indicating the collapse of monolayer is approximately 23 mN/m. On the basis of these results, we hereafter fabricate the pure MS_{18} LB film using the surface pressure of 15 mN/m.

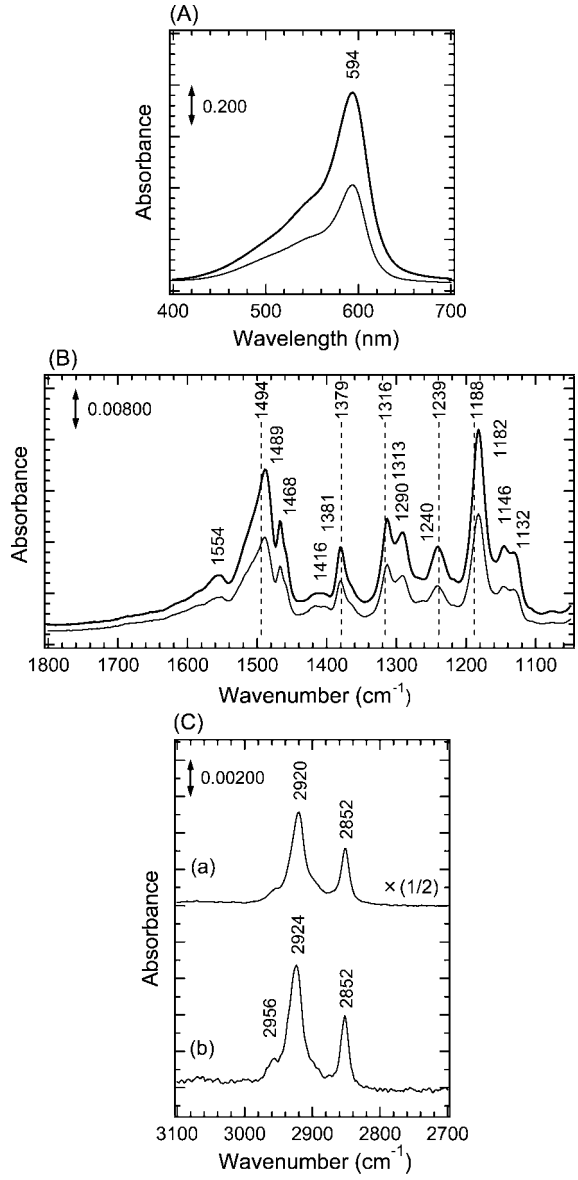

Figure 3. Polarized visible and IR absorption spectra of a pure MS_{18} LB film in the regions of (A) 400−700 nm and (B) 1800−1040 cm^{-1}. The thick and thin lines refer to the polarized spectra $A_{||}$ and $A_{\perp}$, respectively. (C) IR (a) transmission and (b) reflection−absorption spectra in the 3100−2700 cm^{-1} region; the transmission and reflection−absorption spectra were measured using non- and p-polarized light, respectively.

3.2. Structural Characterization of As-Deposited LB Film of Pure MS_{18} System. Figure 3A,B shows polarized transmission absorption spectra in visible and IR fingerprint regions of a pure MS_{18} LB film, respectively. The thick and thin lines correspond to the polarized spectra $A_{||}$ and $A_{\perp}$, respectively. In Figure 3A, the LB film shows a red-shifted sharp absorption band at 594 nm from the MS_{18} monomer peak at around 530 nm and is also associated with a shoulder in the 420−550 nm region. This result is in good agreement with that reported by earlier work.[14] The red-shifted band is ascribed to the J-aggregation, and the shoulder is caused by the formation of $MS_{18}-MS_{18}$ dimer with Davydov splitting.[14] The dichroic ratio $R(=A_{||}/A_{\perp})$ for J-band peak at 594 nm is much greater than unity. The R-value originates from the MS_{18} head-to-tail alignment in J-aggregate and the flow orientation effect of J-aggregate elongated in shape.[12] Then, the size of J-aggregate is on the order of several hundred nanometers (see Supporting Information, Section 1).

In Figure 3B, dotted lines refer to wavenumber positions of the MS_{18} nonaggregation state attained from the result of thermal behavior of J-aggregate in the binary system.[5] Detailed assignments of MS_{18} IR bands are listed in Table 1.[16] Sharp peaks are seen at 1554, 1489, 1381, 1313, 1240, 1182, and 1146 cm^{-1}, and their tendencies of R are similar to that in the visible peak at 594 nm in Figure 3A. These results are also consistent with that reported by earlier study.[14] In the 1800−1700 cm^{-1} region, no peak due to free carboxylic groups of MS_{18} is observed,[5,8−10,13−16,19,22] whereas a fairly small peak assigned to the free keto group of MS_{18} seems to slightly appear near 1680 cm^{-1}, referring to the subsequent result in Figure 6 as well.[5,9,13−16,22] Therefore, it is indicated that the carboxylic group in MS_{18} and the keto group in adjacent MS_{18} in the J-aggregate are coupled by Cd^{2+} one after another.[5,14−16] In addition, the slight peak at around 1680 cm^{-1} suggests the existence of $MS_{18}-MS_{18}$ dimer with Davydov splitting, where two carboxylic groups are connected with Cd^{2+}.[5,14−16] This correspond to the shoulder at 420−550 nm in Figure 3A.[14] Moreover, to be checked is the packing form between MS_{18} hydrocarbon chains. One-single peak, assigned to the mode of CH_2 in-plane bending deformation vibration[13,14,23,24] of the MS_{18} hydrocarbon chain,[5,8−10,16] is observed at 1468 cm^{-1}, suggesting that the chain does not form orthorhombic packing.

The results of IR measurements for MS_{18} chromophores in Figure 3B have been interpreted as follows. The positions of sharp peaks at 1489, 1313, and 1182 cm^{-1} are markedly downward shifted from those of the MS_{18} nonaggregation state. The result is attributed to the increase in the MS_{18} intramolecular charge transfer (see Figure 1) caused by (1) coupling of Cd^{2+} to the MS_{18} chromophore and (2) J-aggregation.[14−16] The MS_{18} intramolecular charge transfer means the delocalization of π-electrons in the butadiene group from the rhodanine to benzothiazolydine groups[5,8−10,14−16,19,22] and in the C═S bond in the rhodanine group in MS_{18}.[5,8−10,16] The MS_{18} intramolecular charge transfer enhanced by the latter case decreases the total energy in the J-aggregation by the resonance effect.[5,8−10,14−16]

Figure 3C, spectra a and b, represent the IR nonpolarized transmission and IR reflection−absorption spectra in the 3100−2700 cm^{-1} region of the pure MS_{18} LB film, respectively. Peaks at 2920 and 2852 cm^{-1} in Figure 3C, spectrum a, and those at 2924 and 2852 cm^{-1} in Figure 3C, spectrum b, are assigned to the CH_2 antisymmetric and symmetric stretching vibration modes[17,23−26] of MS_{18} hydrocarbon chain,[5,8−10,13,22] respectively. These wavenumber positions are upward shifted from those at 2917 and 2849 cm^{-1} whose positions are characteristic of the all-trans conformation of hydrocarbon chain.[8,13,22−26] The results suggest that the gauche conformer is slightly contained in the MS_{18} hydrocarbon chain. Then, we have confirmed that the R-value of transmission spectra is approximately unity, suggesting the uniformly distributed orientation of MS_{18} hydrocarbon chain around the film normal. Furthermore, the long axis of MS_{18} hydrocarbon chain tilts by 25.0° from the film normal (see Supporting Information, Section 2). Therefore, we can recognize that the tilt angle in the pure MS_{18} system fairly approaches the film normal than that (43.5°) in the previous $MS_{18}-C_{20}$ binary system.[5]

3.3. Temperature-Dependent Changes in MS_{18} Aggregation State, Chromophore and Domain Size. Figure 4 depicts temperature-dependent UV−visible absorption spectra of the pure MS_{18} LB film. Figure 5a−c plots the normalized peak

TABLE 1: Wavenumber Positions (cm^{-1}) and Assignment of IR Bands for LB Films of Pure MS_{18} and $MS_{18}-C_{20}$ Binary Systems Prepared under a Subphase Containing a Cadmium (Cd^{2+}) Ion

nonaggregation state[a]	J-aggregate at 25 °C[b]	aggregation state at 150 °C[b]	blue-shifted aggregate at 180 °C[b]	assignment[c]
	1555	(1564)[d]	(1562)[d]	$C_5=C_\beta$, $C_\beta-C_\alpha$, C_4-C_5
1494	1486	1490	1491	$C_\alpha=C_{2'}$, $C_{2'}-N_{3'}$, $\delta(CH_2$-alkyl)
1379	1380	1378	1378	C_2-N_3, benzene ring, $C_{3a}-N_{3'}$
1316	1314	1313	1313	
1239	1240			$C_\alpha=C_{2'}$, C−O, CCH (alkyl)
1188	1183	1184	1182	$C_2=S_{2a}$, C_2-N_3, CCH (benzene)
	1145			

[a] The data were taken from ref 5. These were wavenumber positions of nonaggregation state at 100 °C from the result of thermal behavior of the mixed LB film of MS_{18}-deuterated arachidic acid (C_{20}-*d*) binary system. [b] These wavenumber positions were attained from the zero crossing point of third derivative spectrum using the original spectrum of Figure 8. [c] These were the assignment from the results of ab initio calculation based on the density functional theory (DFT), assuming MS_4 with a butyl group and (π,π,π) conformer in Figure 1 in chloroform solution in ref 16. [d] The reliability of these positions is lower than that of other positions, since the extent of dispersion of positions plotted against temperature was fairly large.

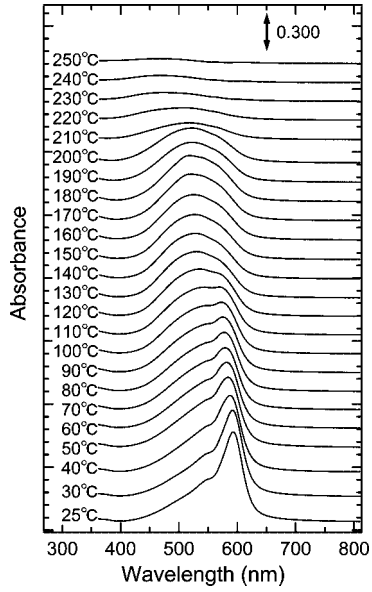

Figure 4. Temperature-dependent UV−visible absorption spectra of the pure MS_{18} LB film (25−250 °C). The spectra are shown every 10 °C from 30 °C in addition to the spectrum measured at 25 °C.

height of absorption maxima, wavelength position of maxima and normalized absorbance at 810 nm in the spectra of Figure 4 as a function of temperature, respectively. The results in Figures 4 and 5 allow us to summarize thermally induced variations. At 25 °C, the J-aggregate is dominantly formed. From 25 to 160 °C, the J-aggregate dissociates gradually, and an inflection point of heights is recognizable at 40 °C. During this temperature region, it seems that both MS_{18} aggregation states of red-shifted and nonaggregation components, more or less, coexist up to 150 °C. Then, a broadband with the maximum at around 530 nm is formed in the range of 150−160 °C. Here, the notable point is that no component near 460 nm is seen from approximately 140 °C due to no presence of $MS_{18}-C_{20}$ monomer in this system, although it is observed in the binary and ternary systems.[5,10] From 160 to 180 °C, blue-shifted peaks appear near 520 nm after the gradual change from 150 to 160 °C. From 180 to 210 °C, the absorption drastically decreases with the wavelength position being located at 525−520 nm. This result is probably caused by the melting phenomenon of MS_{18} chromophores coupled with Cd^{2+}, taking into consideration the melting point (206 °C) investigated by differential scanning calorimeter (DSC) measurement in the $MS_{18}-C_{20}$ binary system as well.[5] (See Supporting Information, Section

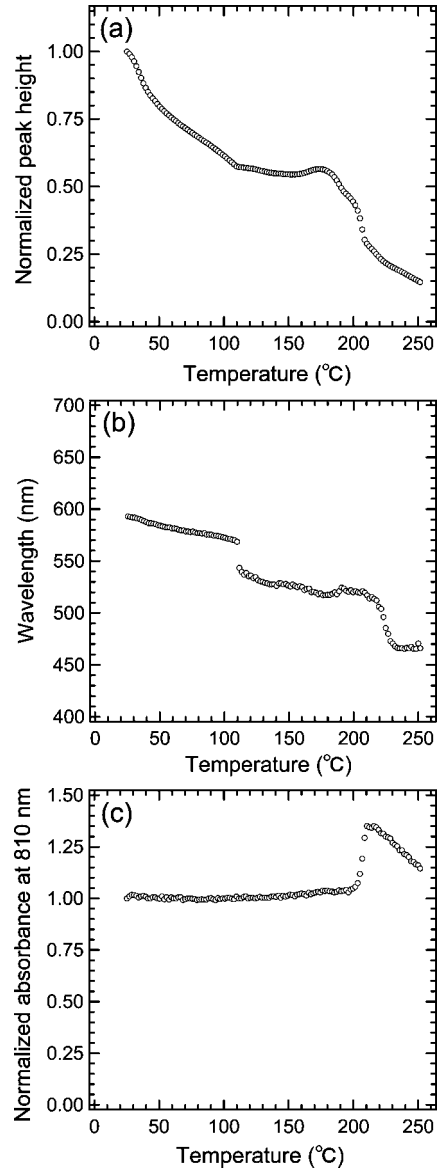

Figure 5. (a) Normalized height of absorption maxima in the UV−visible absorption spectra plotted as a function of temperature. (b) Temperature-dependent changes in wavelength positions of the absorption maxima. (c) Normalized absorbance at 810 nm plotted versus temperature.

3) The diminution of absorption accompanied with the melting of MS_{18} chromophore is attributed to the drastic deviation from

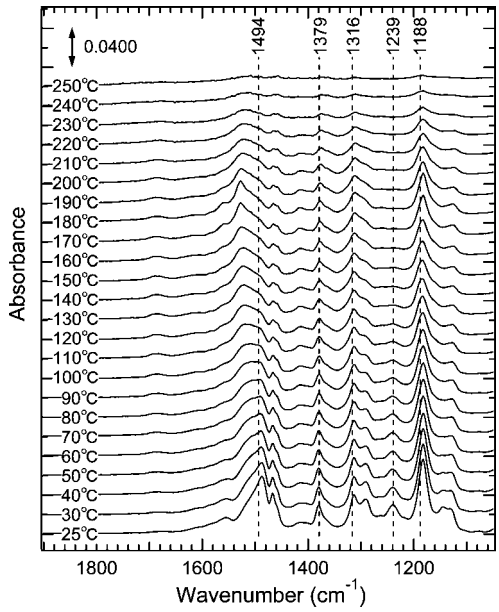

Figure 6. Temperature-dependent IR absorption spectra in the 1800−1040 cm^{-1} region of the pure MS_{18} LB film (25−250 °C).

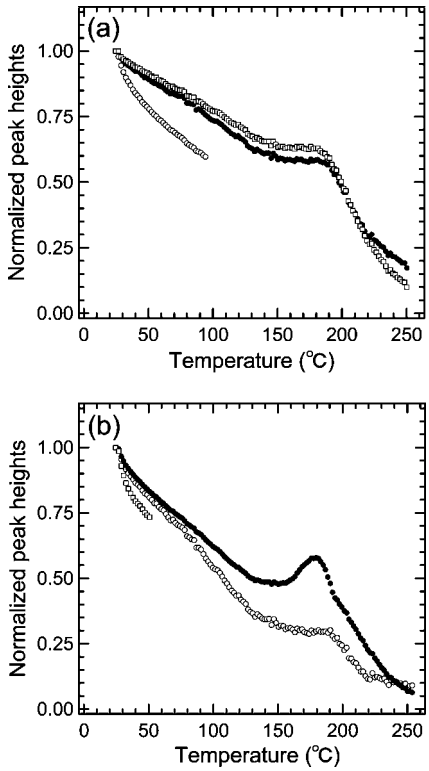

Figure 7. Normalized height of peaks at around (a) 1490 (○), 1380 (●), and 1315 (□) cm^{-1}, and (b) 1240 (○) and 1185 (●), and 1145 (□) cm^{-1} in the IR spectra plotted as a function of temperature.

the in-plane orientation of MS_{18} transition dipole moments. From 210 to 250 °C, the absorption diminishes by degrees, and the peak position shifts from 520 to 470 nm. This is due to the decomposition and/or evaporation of MS_{18} chromophores with Cd^{2+}. In Figure 5c, the baseline shift in the region with no absorption is an indicator of changes in the domain size of crystallites composed of functional molecules, reflecting the phenomenon of diffusion of incident light.[5,10,27] From 25 to 200 °C, the increment of baseline is within 5%. While this result seems to imply no significant change in the size of MS_{18} domain which corresponds to the assemblies of MS_{18} molecules that decrease from the length of J-aggregate, we discuss it in Section 3.4 in more detail, referring to the result of disconnection of Cd^{2+} coupled to MS_{18} as well. Then, the baseline suddenly increases by 30% from 200 to 210 °C and then decreases up to 250 °C. The former result is attributed to the increase in the MS_{18} domain size by the fusion of many MS_{18} assemblies with the melting phenomena, which probably arises from the drastic diminution of grain boundary among many MS_{18} assemblies. On the other hand, the latter one is possibly caused by the decrease in the MS_{18} domain size that increases from 200 to 210 °C, which originates from the subsequent decomposition and/or evaporation of MS_{18} chromophores with the Cd^{2+} ion.

3.4. Temperature-Dependent Variations in Degree of MS_{18} Intramolecular Charge Transfer. Figure 6 shows temperature-dependent IR absorption spectra in the fingerprint region of the pure MS_{18} LB film. From the 1800−1600 cm^{-1} region, we obtain the significant information on the disconnection of Cd^{2+} coupled to MS_{18}. The peak at around 1680 cm^{-1}, assigned to the free keto group of MS_{18},[5,9,10,13−16,19,22] gradually increases from 25 to approximately 200 °C. This result suggests that the coupling of Cd^{2+} to MS_{18} dissociates from the keto group. According to our previous paper,[9] we have reported that the increase in thermal mobility of MS_{18} hydrocarbon chain during secondary treatments probably has the influence on the disconnection of coupling by Cd^{2+} from the keto group in MS_{18} on the basis of the results of variations from H-aggregate by applying heat treatment in air atmosphere (HT) without a continuous scan and hydrothermal treatment in the liquid phase (HTTL). Consequently, we have understood that the disconnection of Cd^{2+} coupling is not the cause but one of the consequences of the diminution in the domain size of MS_{18} aggregates. Referring to these results and interpretation, we can discuss the decrease in the domain size by checking the fluctuation of 1680 cm^{-1} peak in IR spectra of fingerprint region. Consequently, it is suggested that the dissociation of Cd^{2+} in MS_{18} is accompanied with the diminution of MS_{18} domain size, although the result in Figure 5C seemed to imply no variation in the domain size. It is also noted that the shoulder or peak at around 1540−1520 cm^{-1} from 25 to 240 °C mainly arises from the antisymmetric stretching vibration mode of COO^- in MS_{18} chromophore,[23,24] although its peak position and height change depend on temperature. Therefore, we do not discussed the change in these bands, since it is not concerned with the MS_{18} conjugated system or C═S bond.[16]

Figure 7 represents temperature-dependent variations in normalized peak heights near (a) 1490 (○), 1380 (●), and 1315 (□) cm^{-1}, and those at around (b) 1240 (○), 1185 (●) and 1145 (□) cm^{-1}. For the fluctuation of peak heights, there is the following tendency. The heights gradually decrease from 25 to 150 °C and are almost kept constant until approximately 180 °C, except for the temporary increase in the 1185 cm^{-1} band peak from 160 to 180 °C. Then, they diminish rapidly up to 250 °C. Figure 8 refers to temperature-dependent changes in wavenumber positions of peaks near (a) 1490 (○) and 1380 (●) cm^{-1}, (b) 1315 (□) and 1240 (○) cm^{-1}, and (c) 1185 (●) and 1145 (□) cm^{-1}. The following tendency can be recognized for the shifts. (i) While the 1490 cm^{-1} band is upward shifted by 4 cm^{-1} from 25 to 150 °C, the fluctuation of upward and downward shifts for the other bands is within 2 cm^{-1}. (ii) The downward shifts within 2 cm^{-1} are observed from 150 to 180 °C, except for the upward shift by 1 cm^{-1} for the 1490 cm^{-1} band. (iii) From 180 to 250 °C, there is an irregular shift for the 1490, 1380, 1315, and 1185 cm^{-1} bands.

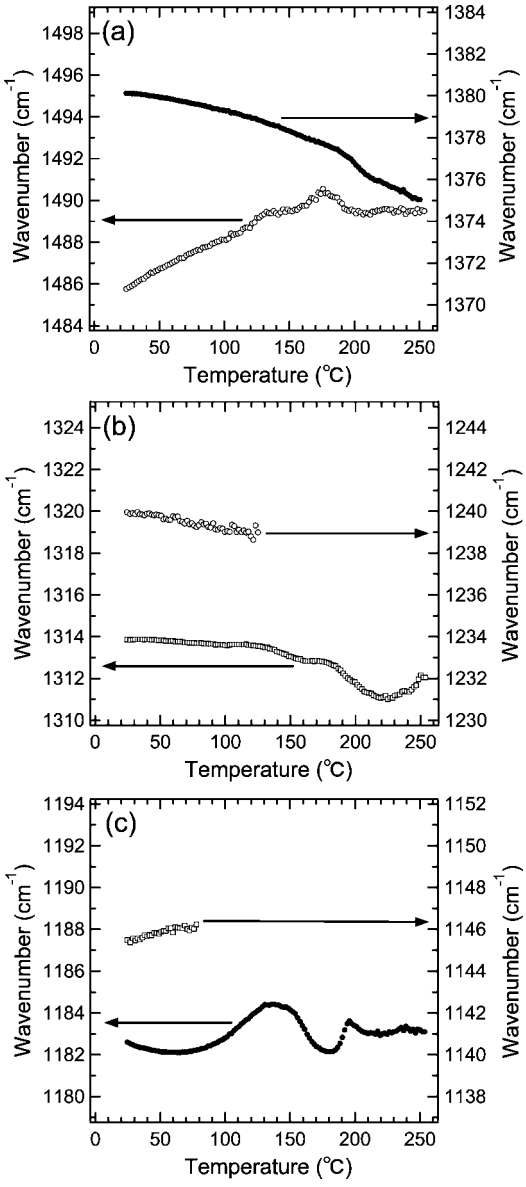

Figure 8. Temperature-dependent changes in wavenumber positions of the peaks at around (a) 1490 (○) and 1380 (●) cm^{-1}, (b) 1315 (□) and 1240 (○) cm^{-1}, and (c) 1185 (●) and 1145 (□) cm^{-1}.

We discuss temperature-dependent variations in the degree of MS_{18} intramolecular charge transfer from the results in Figures 3B, 6, 7, and 8. For the J-aggregation at 25 °C, the MS_{18} intramolecular charge transfer is induced, as described in Section 3.2. The results from 25 to 150 °C are attributed to the gradual decrease in the degree of MS_{18} intramolecular charge transfer. From 150 to 160 °C, the degree of charge transfer of the central conjugated system in MS_{18} is almost unchanged, whereas that of the C═S bond in MS_{18} temporarily increases. The similar tendency continues from 160 to 180 °C as well. From 180 to 250 °C, it is indicated that the degrees in the MS_{18} intramolecular charge transfer decrease dramatically from those at 180 °C.

3.5. Temperature-Dependent Changes in Orientation, Conformation, Thermal Mobility and Packing Nature of MS_{18} Hydrocarbon Chain. Figure 9 depicts temperature-dependent IR spectra in the 3100−2700 cm^{-1} region. Assignments of two peaks are the same as those in Figure 3C, spectrum a, in Section 3.2. In Figure 10a−c, normalized peak heights, wavenumber positions and normalized full width at the half-

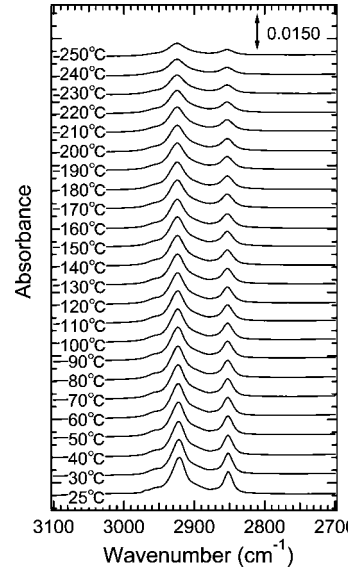

Figure 9. Temperature-dependent IR spectra in the 3100−2700 cm^{-1} region of the pure MS_{18} LB film (25−250 °C).

maxima (fwhm) for the CH_2 antisymmetric (○) and symmetric (●) stretching bands are shown, respectively. From 25 to 40 °C, the heights diminish in Figure 10a. Then, the positions in Figure 10b are gradually upward shifted with a convex curve against temperature, and the fwhm values increase linearly in Figure 10c. Consequently, the height decreases in Figure 10a are probably ascribable not only to the increment of gauche conformation to the MS_{18} hydrocarbon chain but also to the orientation change that the long axis of MS_{18} hydrocarbon chain slightly becomes more parallel to the film surface by the increase in thermal mobility, in comparison with the case at 25 °C. From 40 to 210 °C, the similar and gentle variation continues to occur than that from 25 to 40 °C. From 210 to 250 °C, the heights in Figure 10a rapidly decrease with a convex curve, which possibly comes from phenomena of the decomposition and/or evaporation of hydrocarbon chain of MS_{18} with Cd^{2+}, referring to the melting point (160 °C) of MS_{18} hydrocarbon chain.[5] (See Supporting Information, Section 3) In addition, the consecutive upward shifts can be seen in Figure 10b, suggesting further increase of the gauche conformation in the hydrocarbon chain of MS_{18} that still remains in the LB film. Then, the fwhm value for the CH_2 antisymmetric mode in Figure 10c multiplies linearly, whereas that for the CH_2 symmetric mode increases with a steeper slope from 205 to 250 °C. The steeper slope may reflect the mere increase in the thermal mobility but also the apparent rise associated with the decomposition and/or evaporation of MS_{18} hydrocarbon chain. Finally, the results of no orthorhombic nature between MS_{18} hydrocarbon chains at 25 °C in Section 3.2 and the increment of fwhm values in Figure 10c from 25 to 250 °C suggest that the MS_{18} hydrocarbon chain has the thermal mobility anytime.[28]

3.6. Correlation among MS_{18} Aggregation state, MS_{18} Intramolecular Charge Transfer, and Packing, Orientation, Conformation and Thermal Mobility of MS_{18} Hydrocarbon Chain. The MS_{18} aggregation state in Figures 4 and 5 can be grouped into ranges of (i) 25, (ii) 25−40, (iii) 40−160, (iv) 160−180, (v) 180−210, and (vi) 210 °C or above, whereas the degree of MS_{18} intramolecular charge transfer in Figures 6, 7, and 8 can be categorized into (i) 25, (ii) 25−40, (iii) 40−150, (iv) 150−160, (v) 160−180, (vi) 180−210, and (vii) 210 °C or above. Then, the height changes in Figure 10a can be divided into (i) 25, (ii) 25−40, (iii) 40−210, and (iv) 210 °C or above,

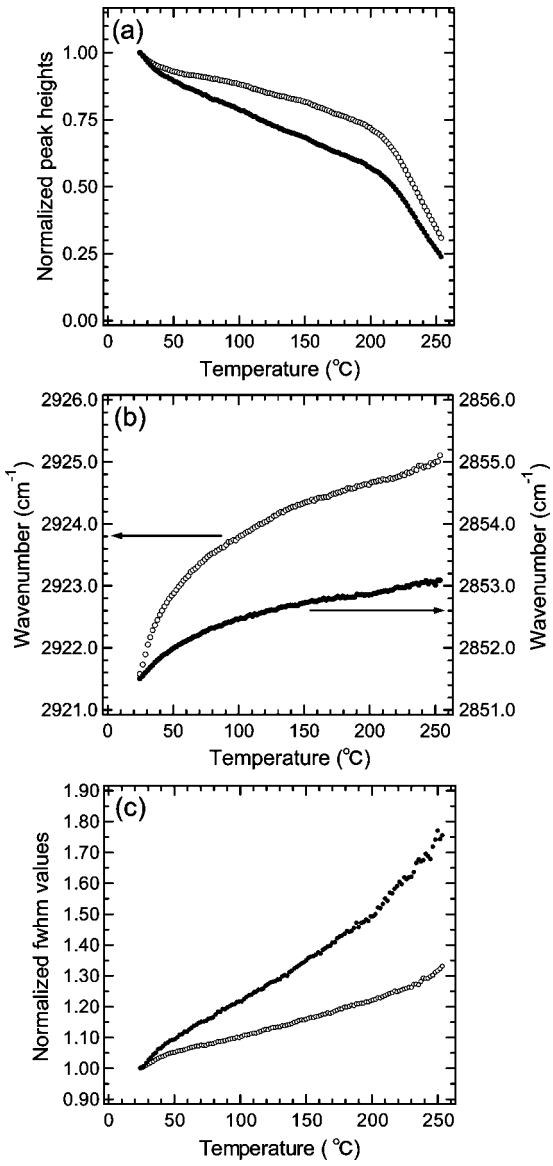

Figure 10. (a) Normalized heights, (b) wavenumber positions, and (c) normalized full width at the half-maxima (fwhm) for peaks at around 2920 (○) and 2850 (●) cm^{-1} in the IR spectra plotted against temperature.

and the variations in fwhm values in Figure 10c can be into (i) 25, (ii) 25−40, (iii) 40−205, and (iv) 205 °C or above. On the other hand, the variation in the conformation in Figure 10b cannot be assorted because of the consecutive upward with a convex curve versus temperature. Referring to the above classification, it is indicated that temperature-dependent changes in the MS_{18} aggregation state in the pure MS_{18} system are closely and mildly linked with the degree of MS_{18} intramolecular charge transfer and the behavior of the packing, orientation, conformation, and thermal mobility of MS_{18} hydrocarbon chain, respectively. While the J-aggregates are similarly formed in both present pure MS_{18} and previous $MS_{18}-C_{20}$ binary systems, the temperature-dependent structural variations of MS_{18} in the pure MS_{18} system are fairly different from those in the binary system. Therefore, it is suggested that the temperature-dependent structural changes in CdC_{20} which is phase-separated from MS_{18} in the binary system have an influence on the degrees of structural variations and linkages in MS_{18}, and the temperature range of linkages. Probably, the similar effect on CdC_{20} would be involved in the previous $MS_{18}-C_{20}-AL_{18}$ ternary system as well.

3.7. Variation in Dissociation Temperature of J-aggregate in Present Pure MS_{18} and Previous Binary Systems and its Origin. The J-aggregate in the pure MS_{18} system dissociates from 25 to 160 °C, and a broadband with the maximum at around 530 nm is formed in the range of 150−160 °C in Figures 4 and 5. Then, the domain size of aggregates also decreases as suggested by Figure 6. Furthermore, the degree of MS_{18} intramolecular charge transfer induced by the J-aggregation diminishes from 25 to 150 °C as demonstrated in Figures 6, 7, and 8. Consequently, the visible band at 530 nm at 150 °C is ascribed to the MS_{18} monomer, based on the results of no shift, broadening and decrease in height in the visible region and also a minimum of degrees of intramolecular charge transfer in the fingerprint region during the decrease in the red-shifted component in the visible region. The dissociation of J-aggregate is due to the increment of thermal mobility of the long axis of MS_{18} hydrocarbon chain suggested by Figure 10c.

As shown in Table 1, the dissociation temperature of J-aggregate in the $MS_{18}-C_{20}$ binary system is lower by 50 °C than that in the pure MS_{18} system.[5] The result is attributed to the fact that the temperature-dependent structural disorder of CdC_{20}, being phase-separated from MS_{18} in the binary system, promotes the dissociation of J-aggregate. Then, the positions in MS_{18} nonaggregation state at 100 °C in the binary system are slightly upward shifted than those at 150 °C in the pure MS_{18} system.[5] In this respect, it is suggested that the chromophore alignments in MS_{18} monomer in the binary system is more disordered than those in the pure MS_{18} system.

3.8. Occurrence of Thermally-Induced Blue-Shifted Band in Pure MS_{18} System and the Switch of Its Driving Force. In Figures 4 and 5, thermally induced blue-shifted bands appear near 520 nm from 160 to 180 °C in the pure MS_{18} system. This result is of great interest, because it contradicts our prediction that a blue-shifted band will not be observed without the driving force by the melting phenomenon of CdC_{20}. The 520 nm band is ascribed to the oligomeric aggregation with MS_{18} side-by-side alignment, based on the increase in the peak height, blue-shift, decrease in the domain size of MS_{18} aggregates, and temporary increment of the degree of charge transfer of C═S bond in MS_{18} respectively suggested by Figures 4−8. The transient increase only in the C═S bond probably induces the stabilization of formation energy of the oligomeric aggregates. This is of great interest, since the degrees of charge transfer not only of the C═S bond but also of the central conjugated system in MS_{18} temporarily and simultaneously multiply when the thermally induced blue-shifted bands in the binary system appear at around 515 nm during 110−160 °C.[5] These results may reflect the difference in the unstableness of MS_{18} geometric structures in the formation of 520 and 515 nm bands. The temperature at which the 520 nm bands come into existence in the pure MS_{18} system is consistent with the melting point (160 °C) of hydrocarbon chain in MS_{18} with Cd^{2+}.[5] Therefore, it is suggested that the partial melting of MS_{18} hydrocarbon chain causes the blue-shifted band at around 520 nm as the driving force, although no dramatic conformation change accompanied by the melting phenomenon of MS_{18} hydrocarbon chain was monitored near 160 °C in IR absorption spectra. Finally, we have a question why thermally induced MS_{18} aggregation is not accompanied by a red-shifted band but a blue-shifted one in the pure MS_{18} and mixed systems. Further studies and discussion to clarify this question will be hereafter needed.

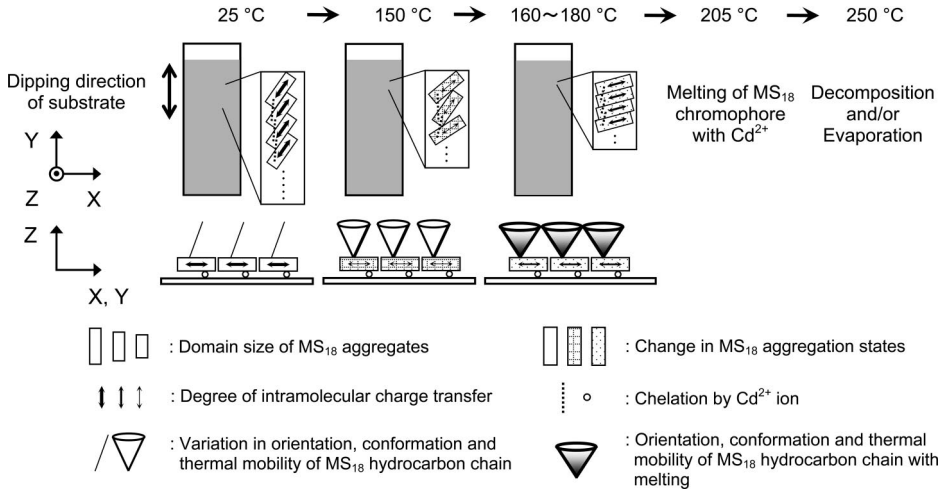

Figure 11. Schematic representation of individual structural changes in MS_{18} aggregates in the pure MS_{18} LB film in the temperature-programmed process of annealing.

3.9. Melting Phenomenon of MS_{18} Chromophore with Cd^{2+} in Pure MS_{18} System, and Reason that Melting Could Not Clearly Be Seen in Mixed Systems. In Figures 4 and 5, the melting phenomenon of MS_{18} chromophores with Cd^{2+} in the pure MS_{18} system is clearly observed at around 205 °C by UV−visible absorption spectra. However, changes associated with the melting could not be detected in the mixed LB films of binary and ternary systems.[5,10] This reason can be comprehended as follows. Since the melting point of CdC_{20} in the mixed LB films is near 110 °C,[5,25] we have discussed that the decomposition and/or evaporation of CdC_{20} should occur at 110 °C or above. If the evaporation arose, the structure of each MS_{18} aggregate in the mixed LB film would be probably damaged. Therefore, it is presumed that the damages are closely concerned with no detection of the melting by UV−visible spectra, even if MS_{18} chromophores with Cd^{2+} melt individually and microscopically. Figure 11 shows schematic representation of individual structural changes in MS_{18} aggregates in the pure MS_{18} LB film in the temperature-programmed process of annealing.

4. Conclusion

In the present study, the structure of MS_{18} J-aggregate in the pure MS_{18} LB film has been characterized, and its thermal behavior has been investigated by UV−visible and IR absorption spectroscopy. The following four road maps have been obtained.

First, it has been indicated that temperature-dependent changes in the MS_{18} aggregation state in the pure MS_{18} system are closely and mildly linked with the degree of MS_{18} intramolecular charge transfer and the behavior of MS_{18} hydrocarbon chain, respectively. Then, it has been suggested from the comparison of results of both present pure MS_{18} and previous $MS_{18}-C_{20}$ binary systems that the temperature-dependent structural changes of CdC_{20}, being phase-separated from MS_{18} in the binary system, have an influence on the degrees of structural variations and linkages in MS_{18}, and the temperature range of linkages.

Second, the J-aggregate in the pure MS_{18} system dissociates from 25 to 150 °C. The dissociation temperature in the pure MS_{18} system is higher by 50 °C than that in the binary system. The difference originates from the fact that the dissociation of J-aggregate in the binary system is promoted by temperature-dependent structural disorder of CdC_{20}.

Third, the 520 nm band occurs in the pure MS_{18} system from 160 to 180 °C. The temperature at which the 520 nm bands appear corresponds to the melting point (160 °C) of MS_{18} hydrocarbon chain, suggesting that the partial melting of MS_{18} hydrocarbon chain induces the 520-nm band as the driving force.

Fourth, the melting of MS_{18} chromophore with Cd^{2+} in the pure MS_{18} system is clearly monitored near 205 °C by UV−visible spectra, whereas that in the previous mixed systems could not be observed. It is expected that the latter no observation is because the evaporation of CdC_{20} gives the structures of individual MS_{18} aggregates the damages, and the damages are strongly related to no detection of its melting phenomenon.

Through the present study, it has been found that the partial melting of octadecyl group in the MS_{18} molecule can produce the order of MS_{18} molecules from monomers to blue-shifted aggregates. This concept may also be useful as one of methods to control the dye aggregation state.

Acknowledgment. The authors are grateful to Dr. Sigeaki Morita, Dr. Akifumi Ikehata, Dr. Yasutaka Kitahama and Dr. Harumi Sato of Kwansei Gakuin University for their valuable comments on the present study. The authors also thank Dr. Masaru Yamashita and Dr. Keiko Tawa of National Institute of Advanced Industrial Science and Technology (AIST) for their support in differential thermal analysis-thermogravimetry (DTA-TG) measurements. This study was supported by "Open Research Center" project (Research Center for Near Infrared Spectroscopy) for private universities; matching fund subsidy was from MEXT (Ministry of Education, Culture, Sport, Science and Technology), 2001−2008. This research was also supported by Izumi Science and Technology Foundation, 2008.

Supporting Information Available: Section 1. The size estimation of J-aggregates by analytical model of flow orientation. Section 2. The determination of orientation of the long axis of MS_{18} hydrocarbon chain in as-deposited LB film of the pure MS_{18} system. Section 3. Differential thermal analysis-thermogravimetry (DTA-TG) measurements of powders of arachidic acid (C_{20}), MS_{18} and merocyanine dye with an ethyl group (MS_2), and differential scanning calorimetry (DSC) measurements of the LB films of pure C_{20} and MS_{18}-C_{20} binary systems coupled with the cadmium (Cd^{2+}) ion. This material is available free of charge via the Internet at http://pubs.acs.org.

References and Notes

(1) (a) Jelley, E. E. *Nature (London)* **1936**, *138*, 1009. (b) Scheibe, G. *Angew. Chem.* **1936**, *49*, 563. (c) *J-Aggregates*; Kobayashi, T., Ed.; World Scientific: Singapore, 1996.

(2) (a) Kuhn, H. *Thin Solid Films* **1989**, *178*, 1. (b) Ulman, A. *An Introduction to Ultrathin Organic Films*; Academic Press, San Diego, CA, 1991. (c) Law, K. Y. *Chem. Rev.* **1993**, *93*, 449. (d) *Organized Monolayers and Assemblies: Structure, Processes and Function, Studies in Interface Science*; Kuroda, S., Moebius, D., Miller, R., Eds.; Elsevier: Amsterdam, 2002; Vol. 16,Chapter 6. (e) Ozaki, Y.; Morita, S.; Hirano, Y.; Li, X. *Monolayer on Air/Solid Interface -Vibrational Spectroscopy and Atomic Force Microscopy,, Advanced Chemistry of Monolayers at Interfaces*; Imae, T., Ed.; Elsevier: Amsterdam, 2007; Chapter 12.

(3) (a) Saito, K. *Jpn. J. Appl. Phys* **1995**, *34*, 3832. (b) Saito, K. *J. Phys. Chem. B* **1999**, *103*, 6579. (c) Saito, K. *J. Phys. Chem. B* **2001**, *105*, 4235. (d) Saito, K.; Kobayashi, S. *Appl. Phys. Lett.* **2002**, *80*, 1489. (e) Wakamatsu, T.; Watanabe, K.; Saito, K. *Appl. Opt.* **2005**, *44*, 906. (f) Zhou, H. S.; Watanabe, T.; Mito, A.; Honma, I.; Asai, K.; Ishigure, K.; Furuki, M. *Mater. Sci. Eng., B* **2002**, *95*, 180. (g) Zhou, H. S.; Watanabe, T.; Mito, A.; Honma, I.; Asai, K.; Ishigure, K. *Mater. Lett.* **2002**, *57*, 589.

(4) (a) Law, K. Y. *J. Phys. Chem.* **1988**, *92*, 4226. (b) Law, K. Y.; Chen, C. C. *J. Phys. Chem.* **1989**, *93*, 2553. (c) Chen, H.; Herkstroeter, W. G.; Perlstein, J.; Law, K. Y.; Whitten, D. G. *J. Phys. Chem.* **1994**, *98*, 5138. (d) Kim, Y. S.; Liang, K. L.; Law, K. Y.; Whitten, D. G. *J. Phys. Chem.* **1994**, *98*, 984. (e) Liang, K.; Law, K. Y.; Whitten, D. G. *J. Phys. Chem.* **1994**, *98*, 13379.

(5) Hirano, Y.; Tateno, S.; Ozaki, Y. *Langmuir* **2007**, *23*, 7003.

(6) Hirano, Y.; Okada, T. M.; Miura, Y. F.; Sugi, M.; Ishii, T. *J. Appl. Phys.* **2000**, *88*, 5194.

(7) Hirano, Y.; Murakami, T. N.; Nakamura, Y. K.; Fukushima, Y.; Tokuoka, Y.; Kawashima, N. *J. Appl. Phys.* **2004**, *96*, 5528.

(8) Hirano, Y.; Tokuoka, Y.; Kawashima, N.; Ozaki, Y. *Vib. Spectrosc.* **2007**, *43*, 86.

(9) Hirano, Y.; Maio, A.; Ozaki, Y. *Langmuir* **2008**, *24*, 3317.

(10) Hirano, Y.; Tateno, S.; Yamashita, Y.; Ozaki, Y. *J. Phys. Chem. B* **2008**, *112*, 14158.

(11) (a) Sugi, M.; Fukui, T.; Iizima, S.; Iriyama, K. *Mol. Cryst. Liq. Cryst.* **1980**, *62*, 165. (b) Nakahara, H.; Fukuda, K.; Moebius, D.; Kuhn, H. *J. Phys. Chem.* **1986**, *90*, 614. (c) Ozaki, Y.; Iriyama, K.; Iwasaki, T.; Hamaguchi, H. *Appl. Surf. Sci.* **1988**, *33*−*34*, 1317. (d) Kuroda, S.; Ikegami, K.; Tabe, Y.; Saito, K.; Saito, M.; Sugi, M. *Phys. Rev. B* **1991**, *43*, 2531. (e) Mouri, S.; Morita, S.; Miura, Y. F.; Sugi, M. *Jpn. J. Appl. Phys.* **2006**, *45*, 7925. (f) Mouri, S.; Moshino, H.; Hasegawa, S.; Miura, Y. F.; Sugi, M. *Jpn. J. Appl. Phys.* **2007**, *46*, 1650. (g) Moshino, H.; Hasegawa, S.; Mouri, S.; Miura, Y. F.; Sugi, M. *Jpn. J. Appl. Phys.* **2008**, *47*, 1034. (h) Yamaguchi, A.; Kometani, N.; Yonezawa, Y. *Thin Solid Films* **2006**, *513*, 125.

(12) Minari, N.; Ikegami, K.; Kuroda, S.; Saito, K.; Saito, M.; Sugi, M. *J. Phys. Soc. Jpn.* **1989**, *58*, 222.

(13) Ikegami, K.; Mingotaud, C.; Delhaès, C. *Phys. Rev. E* **1997**, *56*, 19.

(14) Ikegami, K.; Mingotaud, C.; Lan, M. *J. Phys. Chem. B* **1999**, *103*, 11261.

(15) Ikegami, K.; Mingotaud, C.; Lan, M. *Thin Solid Films* **2001**, *393*, 193.

(16) Ikegami, K.; Kuroda, S. *Chem. Phys.* **2003**, *295*, 205.

(17) Ikegami, K. *J. Chem. Phys.* **2004**, *121*, 2337.

(18) (a) Kato, N.; Saito, K.; Aida, H.; Uesu, Y. *Chem. Phys. Lett.* **1999**, *312*, 115. (b) Kato, N.; Saito, K.; Uesu, Y. *Chem. Phys. Lett.* **2000**, *326*, 395. (c) Kato, N.; Saito, K.; Serata, T.; Aida, H.; Uesu, Y. *J. Chem. Phys.* **2001**, *115*, 1473. (d) Kato, N.; Yuasa, K.; Araki, T.; Hirosawa, I.; Sato, M.; Ikeda, N.; Iimura, K.; Uesu, Y. *Phys. Rev. Lett.* **2005**, *94*, 136404.

(19) Kato, N.; Yamamoto, M.; Itoh, K.; Uesu, Y. *J. Phys. Chem. B* **2003**, *107*, 11917.

(20) Nakahara, H.; Moebius, D. *J. Colloid Interface Sci.* **1986**, *114*, 363.

(21) (a) Ray, K.; Nakahara, H.; Sakamoto, A.; Tasumi, M. *Chem. Phys. Lett.* **2001**, *342*, 58. (b) Murata, M.; Mori, K.; Sakamoto, A.; Villeneuve, M.; Nakahara, H. *Chem. Phys. Lett.* **2005**, *405*, 32. (c) Murata, M.; Villeneuve, M.; Nakahara, H. *Chem. Phys. Lett.* **2005**, *405*, 416.

(22) (a) Fujimoto, Y.; Ozaki, Y.; Takayanagi, M.; Nakata, M.; Iriyama, K. *J. Chem. Soc. Faraday Trans.* **1996**, *92*, 413. (b) Fujimoto, Y.; Ozaki, Y.; Iriyama, K. *J. Chem. Soc., Faraday Trans.* **1996**, *92*, 419.

(23) Umemura, J.; Kamata, T.; Kawai, T.; Takenaka, T. *J. Phys. Chem.* **1990**, *94*, 62.

(24) (a) Hasegawa, T. *J. Phys. Chem. B* **2002**, *106*, 4112. (b) Hasegawa, T. *Anal. Chem.* **2007**, *79*, 4385.

(25) Naselli, C.; Rabolt, J. F.; Swalen, J. D. *J. Chem. Phys.* **1985**, *82*, 2136.

(26) Azumi, R.; Matsumoto, M.; Kuroda, S.; Crossley, M. J. *Langmuir* **1995**, *11*, 4495.

(27) (a) Wang, Y.; Nichogi, K.; Terashita, S.; Iriyama, K.; Ozaki, Y. *J. Phys. Chem. B* **1996**, *100*, 368. (b) Morita, S.; Nichogi, K.; Ozaki, Y. *J. Phys. Chem. B* **2000**, *104*, 1183.

(28) In Figures 3B and 6, peak at 1468 cm^{-1} at 25 °C is assigned to the coupling mode of CH_2 in-plane bending mode of the octadecyl group substituted to MS_{18}, and the acetic acid in MS_{18} chromophore.[16] In addition, the shoulder near 1460 cm^{-1} at the same temperature is identified as the CH_2 in-plane bending mode of the acetic acid in MS_{18} chromophore.[16] Therefore, their two peaks, which can be well recognized from 120 up to 230 °C in Figure 6, suggest no orthorhombic nature between the MS_{18} octadecyl groups.

JP808220W